Commun. Comput. Phys.
doi: 10.4208/cicp.OA-2016-0010

Vol. **21**, No. 2, pp. 515-525
February 2017

Hamiltonian Analysis and Dual Vector Spectral Elements for 2D Maxwell Eigenproblems

Hongwei Yang[1], Bao Zhu[2] and Jiefu Chen[3,*]

[1] *College of Applied Sciences, Beijing University of Technology, Beijing 100124, P.R. China.*
[2] *School of Materials Science and Engineering, Dalian University of Technology, Dalian, Liaoning 116023, P.R. China.*
[3] *Department of Electrical and Computer Engineering, University of Houston, Houston, TX 77004, USA.*

Communicated by Weng Cho Chew

Received 18 January 2016; Accepted (in revised version) 26 August 2016

Abstract. The 2D Maxwell eigenproblems are studied from a new point of view. An electromagnetic problem is cast from the Lagrangian system with single variable into the Hamiltonian system with dual variables. The electric and magnetic components transverse to the wave propagation direction are treated as dual variables to each other. Higher order curl-conforming and divergence-conforming vector basis functions are used to construct dual vector spectral elements. Numerical examples demonstrate some unique advantages of the proposed method.

AMS subject classifications: 35Q61, 65P10, 65N30, 65N25

Key words: Maxwell eigenproblem, Hamiltonian system, symplectic eigenvalue analysis, dual variables, spectral element method.

1 Introduction

2D Maxwell eigenproblem such as the waveguide analysis plays an important role in designing optical and microwave devices including microstrips and optical fibers. Popular finite element methods (FEM) [1–4] for this study are usually based on the second order wave equations with one variable (electric field **E** or magnetic field **H**). Once the FEM process is done and the discretized variable is obtained, numerical differentiation will be needed to calculate the other variable based on a fixed FEM mesh and the Maxwell's equations. Obviously the accuracy of the second variable obtained from this

*Corresponding author. *Email addresses:* yanghongwei@bjut.edu.cn (H. Yang), bzhu@dlut.edu.cn (B. Zhu), jchen84@uh.edu (J. Chen)

post-processing will be one order lower than that of the first variable, and this precision mismatch is undesirable for some applications requiring the values of both electric and magnetic fields simultaneously, e.g., the waveport implementation in time domain finite difference or finite element method. On the other hand, several schemes have been proposed simultaneously using both **E** and **H** as variables [5–8].

In this study we propose a Hamiltonian analysis and a dual vector spectral element method (SEM) for the 2D Maxwell eigenproblems. An electromagnetic problem is cast from the Lagrangian system with single variable into the Hamiltonian system [9], which is based on the transverse electric field and transverse magnetic field as dual variables to each other. Higher order curl-conforming and divergence-conforming vector basis functions based on the Gauss-Lobatto-Legendre (GLL) polynomials [10, 11] are employed to construct the dual vector SEM. The dual vector SEM discretization of an electromagnetic eigenproblem can achieve spectral accuracy with the increase of interpolation degrees of basis functions, and they can directly give the numerical solutions for both electric field and magnetic field at the same level of accuracy.

2 Hamiltonian system and dual variable variational principle

Conventional FEM analysis is usually based on one variable. In other words, it is described in the Lagrangian system. To develop the dual vector SEM in the Hamiltonian system, we need to start with the first order Maxwell's equations

$$\begin{cases} \nabla\times\mathbf{E}=-j\omega\mu\mathbf{H}, \\ \nabla\times\mathbf{H}=j\omega\epsilon\mathbf{E}. \end{cases} \tag{2.1}$$

Here excitation and dissipation terms are omitted without losing the generality of analyzing a eigenproblem. **E** is electric field and **H** is magnetic field. ϵ and μ denote the permittivity and permeability, respectively. The variational form for the above equations is

$$\Pi(\mathbf{E},\mathbf{H})=\int_\Omega\left[\mathbf{H}^*\cdot\nabla\times\mathbf{E}+\frac{j\omega\mu}{2}\mathbf{H}^*\cdot\mathbf{H}+\frac{j\omega\epsilon}{2}\mathbf{E}^*\cdot\mathbf{E}\right]d\Omega,\quad \delta\Pi=0, \tag{2.2}$$

where Ω denotes the area of this eigenproblem, and * is the complex conjugate operator. Performing the variational w.r.t. **E** and **H** independently in (2.2) will lead to the original equations (2.1). The proof steps are straightforward and will not be elaborated here.

To cast (2.2) into the Hamiltonian system we define the transverse electric and magnetic fields as dual variables [9]

$$\mathbf{q}=\mathbf{E}_t,\quad \mathbf{p}=\mathbf{H}_t\times\mathbf{z}, \tag{2.3}$$

where **z** denotes the direction of wave propagation. We also decompose the Nabla operator into transverse and longitudinal components

$$\nabla=\nabla_t+(\cdot)\mathbf{z}, \tag{2.4}$$

where $(\dot{\cdot})$ is defined as $\partial(\,)/\partial z$, e.g. $\dot{\mathbf{q}}=\partial\mathbf{q}/\partial z$. Here we made an analogy between the time and the partial derivative w.r.t. the z direction, and this is to follow the convention in the Hamiltonian mechanics [9]. With (2.3) and (2.4) the functional (2.2) can be rewritten as

$$\Pi=\int_\Omega\Big[\mathbf{p}^*\cdot\dot{\mathbf{q}}+\mathbf{E}_z\cdot(\nabla\cdot\mathbf{p})^*+\frac{j\omega\epsilon}{2}(\mathbf{q}^*\cdot\mathbf{q}+\mathbf{E}_z^*\cdot\mathbf{E}_z) +\mathbf{H}_z^*\cdot\nabla_t\times\mathbf{q}+\frac{j\omega\mu}{2}(\mathbf{p}^*\cdot\mathbf{p}+\mathbf{H}_z^*\cdot\mathbf{H}_z)\Big]d\Omega. \tag{2.5}$$

By performing variational w.r.t. $\mathbf{E}_z$ and $\mathbf{H}_z$, we will get

$$\begin{cases}\mathbf{E}_z=-j\nabla_t\cdot\mathbf{p}/(\omega\epsilon),\\ \mathbf{H}_z=j\nabla_t\times\mathbf{q}/(\omega\mu).\end{cases} \tag{2.6}$$

With substitution (2.6) into (2.5), the dual variable variational principle is as

$$\Pi(\mathbf{q},\mathbf{p})=\int_\Omega[\mathbf{p}^*\cdot\dot{\mathbf{q}}-H(\mathbf{q},\mathbf{p}))]d\Omega,\quad \delta\Pi=0, \tag{2.7}$$

where

$$H(\mathbf{q},\mathbf{p})=-\frac{j\omega\epsilon}{2}\mathbf{q}^*\cdot\mathbf{q}+\frac{j}{2\omega\mu}(\nabla_t\times\mathbf{q})^*\cdot(\nabla_t\times\mathbf{q}) -\frac{j\omega\mu}{2}\mathbf{p}^*\cdot\mathbf{p}+\frac{j}{2\omega\epsilon}(\nabla_t\cdot\mathbf{p})^*(\nabla_t\cdot\mathbf{p}) \tag{2.8}$$

is the Hamiltonian function.

3 Symplectic eigenproblem analysis

Without loss of generality, we can assume boundary is either perfect electric conductor (PEC) or perfect magnetic conductor (PMC). For open region problems, we can always apply a perfectly matched layer (PML) to enclose the cross section and then let the outermost boundary be PEC or PMC. Taking variation for $\mathbf{q}$ and $\mathbf{p}$ in (2.7) separately, with the above boundary conditions and using Green's identities as well as Gauss's theorem, we will obtain dual differential equations as

$$\dot{\mathbf{v}}=\mathbf{H}\mathbf{v}, \tag{3.1}$$

where

$$\mathbf{v}=\begin{bmatrix}\mathbf{q}\\ \mathbf{p}\end{bmatrix} \tag{3.2}$$

and

$$\mathbf{H}=\begin{bmatrix} 0 & -j\omega\mu-\frac{j}{\omega\epsilon}\nabla_t\nabla_t\cdot \\ -j\omega\epsilon+\frac{j}{\omega\mu}\nabla_t\times\nabla_t\times & 0 \end{bmatrix}. \tag{3.3}$$

Assuming γ is the propagation constant along the longitudinal direction, i.e. $\mathbf{v}=\Psi(x,y)\exp(\gamma z)$, (3.1) will be transformed to

$$\mathbf{H}\Psi=\gamma\Psi, \tag{3.4}$$

where γ and Ψ are eigenvalue and eigenvector of this problem.

It is not difficult to prove that (3.4) is a symplectic eigenproblem. For any two vectors Ψ_a and Ψ_b, as long as they satisfy boundary conditions, we can obtain the following identity based on Green's identities and Gauss's theorem

$$\langle\Psi_a,\mathbf{H}\Psi_b\rangle=\langle\Psi_b,\mathbf{H}\Psi_a\rangle, \tag{3.5}$$

where the angle bracket operator means symplectic inner product

$$\langle\Psi_a,\Psi_b\rangle=\int_\Omega\Psi_a\cdot\mathbf{J}\cdot\Psi_b d\Omega \tag{3.6}$$

and $\mathbf{J}$ is a 2×2 unit symplectic matrix

$$\mathbf{J}=\begin{bmatrix} 0 & 1 \\ -1 & 0 \end{bmatrix}. \tag{3.7}$$

Once the identity (3.5) is verified and the the operator matrix $\mathbf{H}$ is proven to be in the Hamiltonian system, there are a series of conclusions of symplectic eigenvalue analysis to be applied to the original Maxwell eigenproblem [9]. For example, if γ is a eigenvalue of the problem, then so will be $-\gamma$. Thus all the eigenvalues can be categorized into two groups:

$$\begin{cases} \gamma_i,\ \ \mathrm{Re}(\gamma_i)<0\ \text{ or }\ \mathrm{Re}(\gamma_i)=0\cap\mathrm{Im}(\gamma_i)<0, \\ \gamma_{-i},\ \ \gamma_{-i}=-\gamma_i,\quad i=1,2,3,\cdots. \end{cases} \tag{3.8}$$

Eigensolutions with $\mathrm{Re}(\gamma_i)=0$ are corresponding to wave propagation, and the others are evanescent modes.

In the Hamiltonian system we have the adjoint symplectic orthogonality

$$\begin{cases} \langle\Psi_i,\Psi_j\rangle=0, \\ \langle\Psi_{-i},\Psi_{-j}\rangle=0, \\ \langle\Psi_i,\Psi_{-j}\rangle=\delta_{ij}, \\ \langle\Psi_{-i},\Psi_j\rangle=\delta_{ij},\quad i>0,\ \ j>0, \end{cases} \tag{3.9}$$

where $\mathbf{\Psi}_i$ and $\mathbf{\Psi}_{-i}$ are eigenvectors corresponding to eigenvalues γ_i and γ_{-i}, respectively. Any field distribution of the 2D Maxwell eigenproblem can be represented by the eigenvectors

$$\begin{cases} \mathbf{v}(x,y)=\sum\limits_{i=1,2,\cdots}(a_i\mathbf{\Psi}_i+b_i\mathbf{\Psi}_{-i}), \\ a_i=-\langle\mathbf{\Psi}_{-i},\mathbf{v}\rangle, \quad b_i=\langle\mathbf{\Psi}_i,\mathbf{v}\rangle. \end{cases} \tag{3.10}$$

The analytical symplectic eigenproblem analysis only applies to very limited geometries filled with homogeneous material. For more general problems, finite elements can be used for discretization. The symplectic operator matrix **H** will become a discretized Hamiltonian matrix after FEM discretization, and (3.4) will be transformed into a Hamiltonian matrix eigenvalue problem.

4 Dual vector spectral elements

Here we propose a dual vector spectral element method for the 2D Maxwell eigenproblem analysis. The mixed-order curl-conforming vector spectral basis function and the mixed-order divergence-conforming vector spectral basis functions are employed to discretize the dual variables **q** and **p** [12–15], respectively. The spectral basis functions are special types of higher order basis functions with sampling points defined as the Gauss-Lobatto-Legendre (GLL) points, which are roots of the derivatives of the GLL polynomials. By choosing GLL points rather than equal-spaced grids as sampling points, the spectral element can avoid the well-known Runge phenomenon and achieve spectral accuracy, which means the numerical results will converge exponentially as the increase of interpolation order of basis functions.

Fig. 1 shows schematics of a third order spectral element for the dual variables. The basis function of the 2D mixed-order curl-conforming vector spectral element is defined as

$$\begin{cases} \mathbf{N}_q^{\xi}(\xi,\eta)=\hat{\xi}\phi_m^{(M-1)}(\xi)\phi_l^{(M)}(\eta), \\ \mathbf{N}_q^{\eta}(\xi,\eta)=\hat{\eta}\phi_m^{(M)}(\xi)\phi_l^{(M-1)}(\eta), \end{cases} \tag{4.1}$$

and the basis function of the 2D mixed-order divergence-conforming vector spectral element is defined as

$$\begin{cases} \mathbf{N}_p^{\xi}(\xi,\eta)=\hat{\xi}\phi_m^{(M)}(\xi)\phi_l^{(M-1)}(\eta), \\ \mathbf{N}_p^{\eta}(\xi,\eta)=\hat{\eta}\phi_m^{(M-1)}(\xi)\phi_l^{(M)}(\eta), \end{cases} \tag{4.2}$$

where ξ and η are variables in the reference coordinate system: $(\xi,\eta)\in[-1,1]\times[-1,1]$. $\hat{\xi}$ and $\hat{\eta}$ are unit vectors in the reference coordinate system.

$$\phi_m^{(M)}(\xi)=\frac{-(1-\xi^2)L'_M(\xi)}{M(M+1)L_M(\xi_m)(\xi-\xi_m)}, \quad m=0,\cdots,M, \tag{4.3}$$

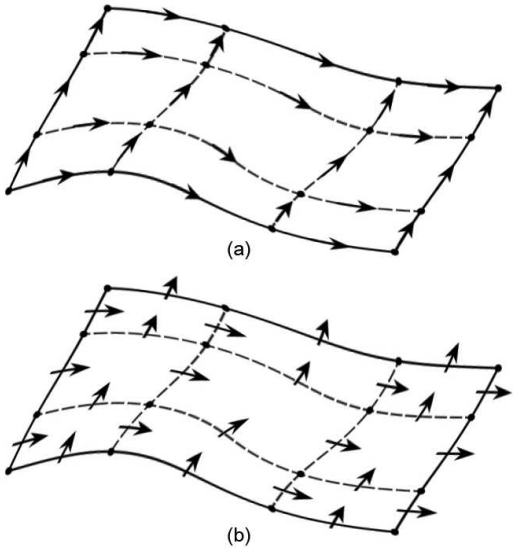

Figure 1: Schematics of 2D dual vector spectral elements: the mixed-order curl-conforming spectral basis function shown in (a) is used to represent $\mathbf{q}$; the mixed-order divergence-conforming spectral basis function shown in (b) is used to represent $\mathbf{p}$. $M=3$ is assumed in this figure.

$L_M(\xi)$ is the Legendre polynomial of degree of M, and ξ_m is chosen as the roots of $(1-\xi_m^2)L'_M(\xi_m)=0$. $\phi_l^{(M)}(\eta)$ is similar to $\phi_m^{(M)}(\xi)$ but for a different coordinate variable.

The dual vector spectral elements need to be mapped to the physical domain with curved edges after its original construction in the reference domain. To maintain the curl-conforming or divergence-conforming properties, co-variant and contra-variant transformations should be applied to the dual variables $\mathbf{q}$ and $\mathbf{p}$, respectively. Details are referred to [14] and not elaborated here.

Assuming k_z as the propagation constant along the z direction, and representing dual variables $\mathbf{q}$ and $\mathbf{p}$ in each element as

$$\mathbf{q}^e=\sum \mathbf{N}_q q^e=\{\mathbf{N}_q\}^T\{q^e\}, \tag{4.4}$$

$$\mathbf{p}^e=\sum \mathbf{N}_p p^e=\{\mathbf{N}_p\}^T\{p^e\}, \tag{4.5}$$

where $\mathbf{q}^e$ and $\mathbf{p}^e$ mean values of dual variables in one element. $\{q^e\}$ and $\{p^e\}$ are vectors of coefficients of corresponding finite element basis functions.

Functional (2.7) will be discretized as

$$\begin{aligned}\Pi=&\frac{1}{2}\sum_e\{q^e\}^H(\mathbf{K}^e_{qq}/\omega-\omega\mathbf{M}^e_{qq})\{q^e\}+\sum_e k_z\{p^e\}^H\mathbf{M}^e_{pq}\{q^e\}\\&+\frac{1}{2}\sum_e\{p^e\}^H(\mathbf{K}^e_{pp}/\omega-\omega\mathbf{M}^e_{pp})\{p^e\},\end{aligned} \tag{4.6}$$

where H denote conjugate transpose, and matrices in (4.6) are

$$\mathbf{K}^e_{qq} = \int\int_{\Omega^e} \frac{1}{\mu^e} \left\{ \nabla_t \times \mathbf{N}^e_q \right\} \cdot \left\{ \nabla_t \times \mathbf{N}^e_q \right\}^T d\Omega, \tag{4.7}$$

$$\mathbf{M}^e_{qq} = \int\int_{\Omega^e} \epsilon^e \left\{ \mathbf{N}^e_q \right\} \cdot \left\{ \mathbf{N}^e_q \right\}^T d\Omega, \tag{4.8}$$

$$\mathbf{K}^e_{pp} = \int\int_{\Omega^e} \frac{1}{\epsilon^e} \left\{ \nabla_t \cdot \mathbf{N}^e_p \right\} \cdot \left\{ \nabla_t \cdot \mathbf{N}^e_p \right\}^T d\Omega, \tag{4.9}$$

$$\mathbf{M}^e_{pp} = \int\int_{\Omega^e} \mu^e \left\{ \mathbf{N}^e_p \right\} \cdot \left\{ \mathbf{N}^e_p \right\}^T d\Omega, \tag{4.10}$$

$$\mathbf{M}^e_{pq} = \int\int_{\Omega^e} \left\{ \mathbf{N}^e_p \right\} \cdot \left\{ \mathbf{N}^e_q \right\}^T d\Omega, \quad \mathbf{M}^e_{qp} = \mathbf{M}^{eT}_{pq}. \tag{4.11}$$

Assembling the above elemental matrices and using the Ritz method, we will obtain the discretized linear system of matrix equations by the dual vector SEM

$$\begin{bmatrix} \mathbf{K}_{qq}/\omega - \omega \mathbf{M}_{qq} & k_z \mathbf{M}_{qp} \\ k_z \mathbf{M}_{pq} & \mathbf{K}_{pp}/\omega - \omega \mathbf{M}_{pp} \end{bmatrix} \begin{bmatrix} \mathbf{q} \\ \mathbf{p} \end{bmatrix} = \begin{bmatrix} \mathbf{0} \\ \mathbf{0} \end{bmatrix}. \tag{4.12}$$

System (4.12) can be used in two ways: in the first scenario the propagation constant k_z is assumed, and the corresponding working frequencies are to be calculated; in the other case the frequency ω will be a fixed value, and the system of equations can be rewritten as a generalized eigenvalue problem with propagation constant as its eigenvalues. Examples of both scenarios will be given and discussed in the following section.

5 Numerical results and discussions

The first example is about a 1 cm$\times$0.4 cm rectangular waveguide filled with air and enclosed by perfect electric conductor. An orthogonal and uniform 4 by 4 SEM mesh with different interpolation order is used to discretize the computational domain, and to calculate the cut-off frequencies of first several modes. Fig. 2 show the relative errors of cut-off frequencies of the first two TE modes and first two TM modes by dual vector SEM with different interpolations orders. We can clearly see that the numerical errors decrease exponentially with the increase of interpolation order. In other word, the dual vector SEM can achieve spectral accuracy. The CPU time and memory consumption of dual vector SEM with different interpolation orders are listed in Table 1, from which we can observe that the computational costs grow rapidly with the increase of order of basis functions, and this is common in higher order finite element schemes. On the other hand, the numbers given in Table 1 are for solving the full eigenproblem of each dual vector SEM scheme. The CPU time as well as memory cost will be much less, and their increasing trends will be much slower if only first several modes (e.g. the first two TE and first two TM modes as shown in Fig. 2) need to be obtained.

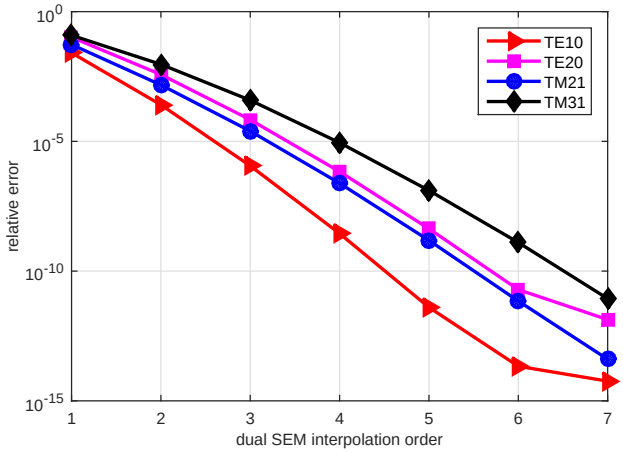

Figure 2: The relative errors of cut-off frequencies by dual vector SEM decrease exponentially with the increase of interpolation orders.

Table 1: Computational costs of dual vector SEM with different interpolation order.

dual SEM order	1st	2nd	3rd	4th	5th	6th	7th
CPU time (s)	0.06	0.11	0.17	0.59	3.44	13.32	37.53
memory (kB)	11	106	540	1,836	4,635	9,878	18,680

2D Maxwell eigenanalysis is an essential step of the waveport implementation in time domain finite different or finite element method, where the transverse components of both electric and magnetic fields are needed for the cross section of a waveport. Conventional FEM is based on one variable, for example, the electric field **E**. The other field **H** needs to be obtained by numerical differentiation based on a fixed FEM mesh, and its accuracy will be one order lower than **E** field directly from the FEM calculation. Apparently this precision mismatch is undesirable to the waveport implementation as well as other applications requiring both fields simultaneously. On the other hand, the dual vector SEM employs interpolation functions of the same degree for both variables, so it guarantee the calculated **E** and **H** fields have the same level of accuracy. Fig. 3 shows the convergence curves of numerical **H** field of the TM21 mode by conventional higher order FEM using **E** as the variable and the proposed scheme based on dual variables. It is clearly to see that the dual vector SEM is one order more accurate than the conventional FEM.

The second example is a shielded microstrip line as shown in Fig. 4. The upper half of this microstrip line is filled with air, and the lower half filled with anisotropic medium $\epsilon_x = \epsilon_y = 9.4$ and $\epsilon_z = 11.6$. Fig. 5 shows the calculated dispersion characteristics of this microstrip line by the proposed dual vector SEM as well as the reference results obtained from a commercial software with a very fine mesh. From this figure we can see that the

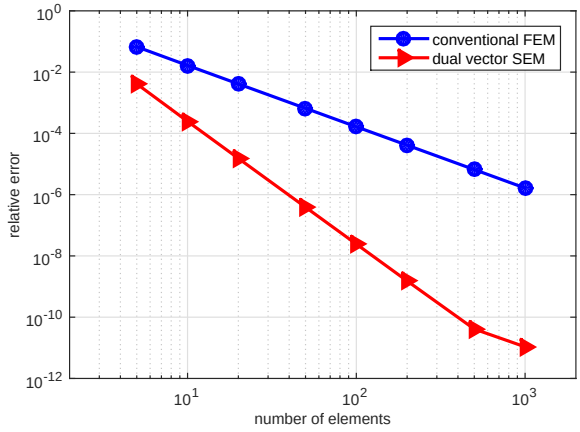

Figure 3: The relative errors of the numerical $\mathbf{H}$ fields of the TM21 mode by second order conventional FEM and second order dual vector SEM.

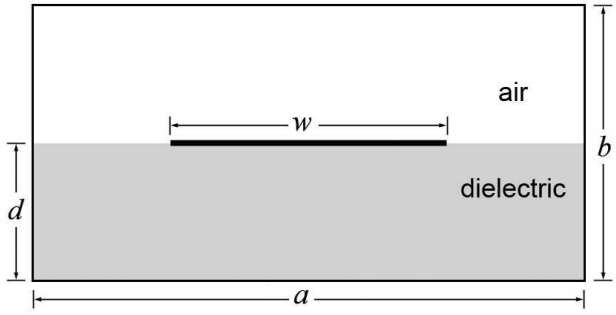

Figure 4: A shield microstrip line with dimension as $a=2b=2w=4d$.

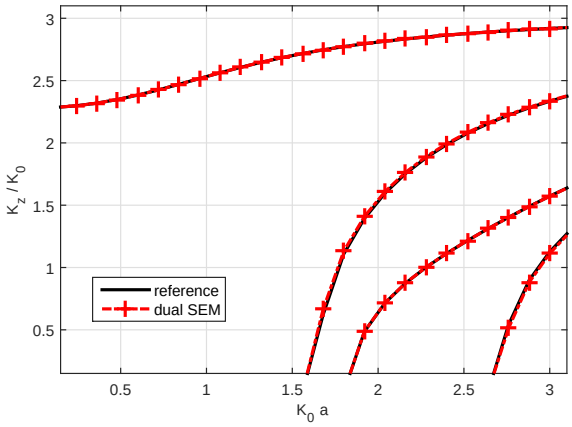

Figure 5: The dispersion characteristics of the first four modes.

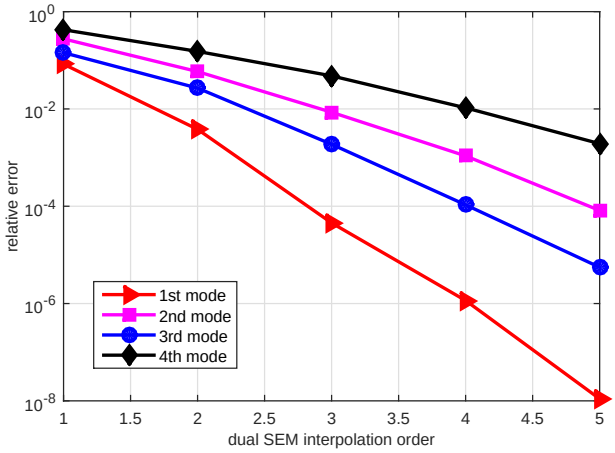

Figure 6: The relative error of the first four modes by dual vector SEM decrease exponentially with the increase of interpolation orders.

dual vector SEM results agree with reference very well. The convergence trends of the first four modes w.r.t. the interpolation order of the dual vector SEM are shown in Fig. 6, from which we again observe the spectral convergence.

6 Conclusion

In this paper we have discussed Hamiltonian analysis for Maxwell eigenvalue problems, and proposed a dual vector spectral element method for numerical calculation. Numerical results demonstrate that the dual vector SEM can simultaneously give numerical results for both electric field and magnetic field with a similar level of accuracy, and it can achieve spectral accuracy with the increase of interpolation degrees of basis functions.

Acknowledgments

The author would like to the reviewers and editors for their constructive comments leading to improvements of this paper. This work was supported by the National Natural Science Foundation of China (Grant Nos. 11172008, 11272020, and 51401045).

References

[1] J. M. Jin, *The Finite Element Method in Electromagnetics*, John Wiley & Sons, 2014.
[2] M. Israel and R. Miniowitz, "An efficient finite-element method for nonconvex waveguides based on Hermitian polynomials," *IEEE Trans. Microw. Theory Techn.*, vol. 35, no. 6, pp. 10191026, Nov. 1987.

[3] J. F. Lee, D. K. Sun, and Z. J. Cendes, "Full-wave analysis of dielectric waveguides using tangential vector finite elements," *IEEE Trans. Microw. Theory Techn.*, vol. 39, no. 8, pp. 1262-1271, Aug. 1991.
[4] L. Z. Zhou and L. E. Davis, "Finite element method with edge elements for waveguides loaded with ferrite magnetized in arbitrary direction," *IEEE Trans. Microw. Theory Techn.*, vol. 44, no. 6, pp. 809-815, Jun. 1996.
[5] K. Radhakrishnan, and W. C. Chew, "Efficient analysis of waveguiding structures," Chapter 10, Fast and Efficient Algorithms in Computational Electromagnetics, W. C. Chew, J. M. Jin, E. Michielssen, and J. Song, Artech House, 2001
[6] J. Chen, B. Zhu, and W. X. Zhong, "Semi-analytical dual edge element method and its application to waveguide discontinuities," *Acta Phys. Sin.*, vol. 58, no. 2, pp. 1091-1099, Feb. 2009.
[7] J. Chen, B. Zhu, and W. X. Zhong, "A dual vector spectral element method for waveguide analysis," IEEE International Conference on Microwave Technology & Computational Electromagnetics, pp. 398-401, Beijing, 2011.
[8] Q. Dai, W. C. Chew, and L. J. Jiang, "Differential forms inspired discretization for finite element analysis of inhomogeneous waveguides," *Prog. Electromagn. Res.*, vol. 143, pp. 745760, 2013.
[9] W. X. Zhong, *Duality System In Applied Mechanics And Optimal Control*, Kluwer, 2004.
[10] L. E. Garcia-Castillo, M. Salazar-Palma, and T. K. Sarkar, "Third-order Nédélec curl-conforming finite element," *IEEE Trans. Magn*, vol. 38, no. 5, pp. 2370-2372, Sept. 2002.
[11] J. H. Lee, T. Xiao, and Q. H. Liu, "A 3-D spectral-element method using mixed-order curl conforming vector basis functions for electromagnetic fields," *IEEE Trans. Microw. Theory Techn.*, vol. 54, no. 1, pp. 437444, Jan. 2006.
[12] J. C. Nédélec, "Mixed finite elements in $\mathbb{R}^3$," *Numer. Math.*, vol. 35, no. 3, pp. 315-341, Mar. 1980.
[13] J. C. Nédélec, "A new family of mixed finite elements in $\mathbb{R}^3$," *Numer. Math.*, vol. 50, no. 1, pp. 57-81, Jan. 1986.
[14] A. F. Peterson, S. L. Ray, and R. Mittra, Computational Methods for Electromagnetics, IEEE Press, 1998.
[15] J. Chen, B. Zhu, W. X. Zhong, and Q. H. Liu, "A semianalytical spectral element method for the analysis of 3-D layered structures," *IEEE Trans. Microw. Theory Techn.*, vol. 59, no. 1, pp. 1-8, Apr. 2011.